Advances in deformation and failure models for concrete

Advances in Deformation and Failure Models for Concrete

Développement dans le domaine des modèles de déformation et de rupture pour le béton

Entwicklungen auf dem Gebiete der Verformungs- und Bruchmodelle für Beton

ZDENĚK P. BAŽANT
Professor of Civil Engineering
Northwestern University
Evanston, IL, USA

SUMMARY
Presented is a non-exhaustive survey of recent advances in mathematical models for nonlinear multi-axial deformation of concrete, the short-time viscoelastic effects, the deformations due to cracks, the overall deformation of cracked concrete and the propagation of crack bands. Emphasis is placed on the treatment of fundamental phenomena such as internal friction and dilatancy due to shear, the interlocking of crack surfaces, and the propagation of crack bands. A new model for the strain-rate effect is presented. Numerical applications are discussed, especially for finite element analysis, and illustrative examples are cited.

RESUME
L'article présente les récents développements des modèles mathématiques pour les déformations non-linéaires et multiaxiales du béton, les effets visco-élastiques instantannés, l'influence des fissures sur les déformations, l'état de déformation en stade fissuré et le développement des zones fissurées. L'accent est mis sur le traitement des phénomènes fondamentaux comme la friction interne et le glissement dû au cisaillement, l'imbrication des surfaces de fissuration et le développement des zones fissurées. Un nouveau modèle pour l'influence de la vitesse des allongements sur les contraintes est également présenté. Des applications numériques, concernant plus spécialement l'analyse par les éléments finis, sont aussi discutées et quelques exemples présentés.

ZUSAMMENFASSUNG
In diesem Beitrag wird ein Überblick über die neuesten Entwicklungen mathematischer Modelle für das nichtlineare, mehrachsige Verformungsverhalten von Beton gegeben: das viscoelastische Kurz-zeitverhalten, der Einfluss der Risse auf die Verformungen, der Verformungszustand in einem gewissen Stadium. Es wird im besonderen eingegangen auf einige grundlegende Probleme, wie die innere Reibung und Schiebung infolge Scherkraft, die Verzahnung von Rissequerschnitten und die Ausbreitung von Rissezonen. Ein neues Modell für das Spannungs-Dehnungs-Zeit-Verhalten wird vorgestellt. Anschliessend werden kurze Anwendungsbeispiele numerisch durchgerechnet und erläutert, insbesondere im Hinblick auf eine Behandlung mittels finiter Elemente.

1.   INTRODUCTION

At the present time we are witnessing rapid advances in the mechanics of con-
crete structures. We are discovering general laws governing the behavior of
these structures and building mathematical models to predict this behavior.
The subject is being placed on a firm scientific basis. The reason for this
development is two-fold: first, more realistic and more accurate predictions
of structural performance are needed to improve the safety, serviceability
and economy of the structures as well as to enable safe and economic design
of new types of concrete structures such as nuclear reactor vessels and con-
tainments, ocean structures, very large span bridges and very tall buildings,
etc; second, we must recognize that this development is being stimulated and
in fact made possible by the availability of powerful computation tools, es-
pecially the finite element method. Without the availability of these tools,
which was the situation not so long ago, development of sophisticated models
for concrete structures would have been practically useless.

Significant advances have recently been made in various directions
including (a) nonlinear triaxial models for solid concrete, (b) fracture of
concrete and behavior of cracked concrete, (c) concrete creep, (d) thermal
effects, (e) moisture effects, (f) chemical effects and corrosion, (g) prob-
abilistic aspects. The spectrum of recent developments in these subjects is
too broad to permit their exposition in a single lecture. Therefore, we must
limit our scope and we will concentrate our attention to nonlinear triaxial
behavior and cracking. In a little more detail we will treat the question of
strain-rate effect and short-time viscoelasticity in triaxial deformation, in
order to use this opportunity to present some known results not yet published.

No claims for the completeness of the present survey are made. In fact, the
survey which follows is rather selective and emphasizes the contributions in
which the writer was directly involved or with which he is closely familiar.
These are mostly the contributions made at Northwestern University and also
some made at Argonne National Laboratory.

2.   NONLINEAR TRIAXIAL BEHAVIOR OF SOLID CONCRETE

2.1.   Friction and Dilatancy

Friction is one of the most difficult features in constitutive modeling. It
leads to violation of the basic stability postulate, namely Drucker's postu-
late [1-4], which serves as the basis for the flow rule of incremental plas-
ticity (normality rule). This postulate is expressed by the condition

$$\Delta W = \frac{1}{2} d\sigma_{ij} d\epsilon_{ij}^{p\ell} > 0 \tag{1}$$

in which ΔW represents the dissipated second order work during a cycle of
applying and removing stress increments $d\sigma_{ij}$, and $d\epsilon_{ij}^{p\ell}$ are the increments of
plastic strains. This postulate is known to constitute a sufficient but not
necessary condition for local stability of the material.[1] Thus, its violation
does not necessarily imply instability, which is a fact often forgetten by
numerical analysts, many of whom insist on using numerical models with symmetric
equation systems which are guaranteed if the postulate is satisfied. It has
been, however, shown [e.g., 15] that inequality (1) may be violated due to in-
ternal friction without causing an instability of the material. It is, there-
fore of considerable interest to find a more general inequality which indicates

---
[1]See [1, 2, 15, 16, 18]

the admissible stable frictional deformations. It has recently been found [5] that the material is stable if the following inequality

$$\Delta W - \chi \, \Delta W_f > 0 \tag{2}$$

is satisfied for any value of χ between 0 and 1; $0 \leq \chi \leq 1$. Here ΔW_f represents what can be called a frictionally blocked elastic energy, expressed as

$$\Delta W_f = \frac{\beta' - \beta^*}{2C} \, d\sigma (d\bar{\tau} + \beta^* d\sigma) \tag{3}$$

in which C, β' and β^* are expressed in terms of the loading function. Although the expressions for a completely general loading function are possible [5], we consider loading functions of the form [27]

$$F(\sigma, \bar{\tau}, \hat{\gamma}^{p\ell}) = 0 \tag{4}$$

in which σ represents the mean (hydrostatic) stress, $\sigma = \sigma_{kk}/3$; $\bar{\tau}$ = stress intensity = $(e_{ij}e_{ij}/2)^{\frac{1}{2}}$ where e_{ij} = deviator of strain tensor ϵ_{ij}; and $\hat{\gamma}^{p\ell}$ = length of the path traced in the space of plastic strains, which is used as a hardening parameter. Tensorial subscripts refer to cartesian coordinates x_i (i = 1,2,3) and repetition of subscripts implies summation. The constants in Eq. 3 are now expressed as [5]:

$$C = -k_1 \frac{\partial F/\partial \hat{\gamma}^{p\ell}}{\partial F/\partial \bar{\tau}} \, , \qquad \beta' = \frac{\partial F/\partial \sigma}{\partial F/\partial \bar{\tau}} \, , \qquad \beta^* = k_2 \frac{de^{p\ell}}{d\hat{\gamma}^{p\ell}} \tag{5}$$

Their meaning may be illustrated taking recourse to Mandel's example [15] (Fig. 1) of a frictional block resting on a rough surface, loaded by a vertical force simulating hydrostatic stress σ, and also subjected to force F from a horizontal spring such that the sliding of the block is imminent. An applied horizontal force on the block simulates $d\bar{\tau}$. Mandel showed that if a disturbing force $d\sigma_{ij}$ inclined from the vertical to the left by an angle less than the friction angle is applied, a sliding of the block results but the block remains stable because it slides only an infinitesimal distance to the right. Yet, Drucker's postulate (Eq. 1) is violated for this movement. Inequality (2) is, however, not violated and coefficient C from this inequality (Eq. 3) represents the spring constant, coefficient β' is the friction coefficient of the block, and β^* is the dilatancy angle indicating the ratio of lifting of the block to its sliding. Coefficients k_1 and k_2 in Eq. 5 are not illustrated by this example and depend on the direction of loading in stress and strain spaces [5].

The usefulness of the new, more general condition sufficient for material stability (Eqs. 2,3) is that it is possible to formulate a frictional constitutive relation and check whether it guarantees stability. Furthermore, by pursuing the same line of reasoning as in classical incremental plasticity, one can derive the flow rule associated with this inequality. It appears that this flow rule allows certain, but not arbitrary, violations of normality of the plastic strain increment vector to the current loading surface. For example it is found [5] that in the plane of $\bar{\tau}$ versus σ the admissible load increment vectors can deviate from the normal to the right and fill a fan of directions, the limiting inclined direction being uniquely determined by the loading surface. The resulting flow rule is, however, totally different from non-associated plasticity because a single loading surface is used and because, in contrast to non-associated plasticity, stability of the material is guaranteed,
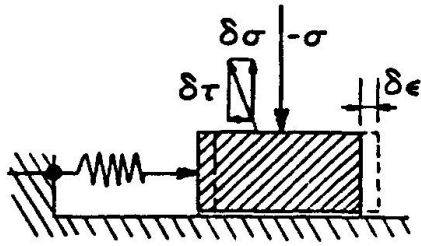
Fig. 1 Example of Spring
Loaded Frictional Block
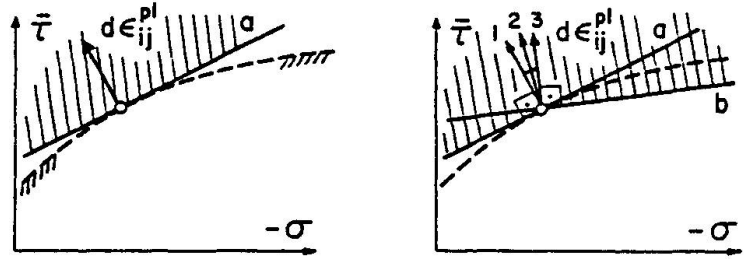
Fig. 2 Plastic Strain Increment Relative
to Loading Surface [5]

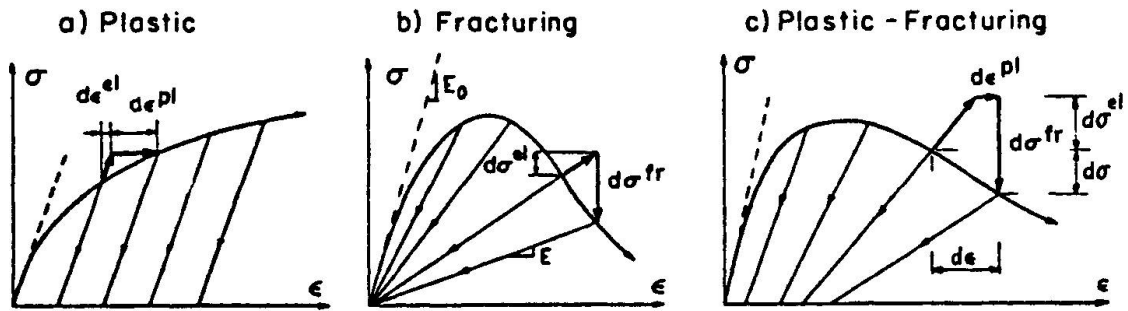a) Plastic   b) Fracturing   c) Plastic - Fracturing

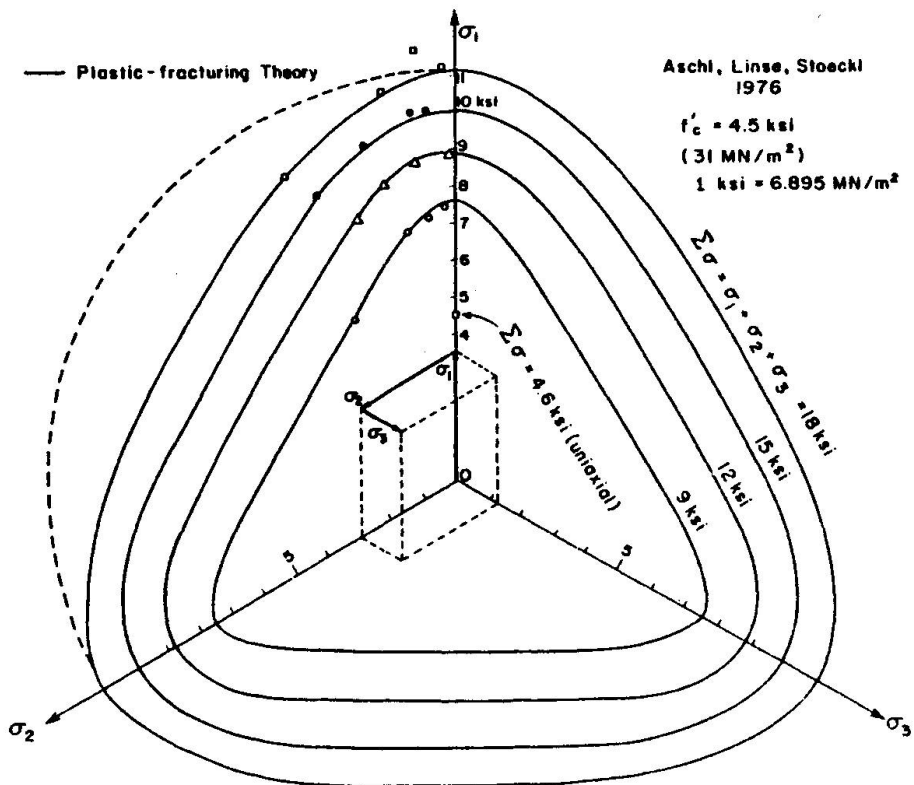**Fig. 3** Characteristic Unloading Behavior

Fig. 4 Failure Envelopes for Plastic-Fracturing Theory whose Loading
Surface Does not Involve Third Invariants

and also becuase the limiting inclined direction of the fan (Fig. 2) depends on the previous loading history and the hardening or softening properties of the material.

Inequality (2) involves only the friction in deviatoric shear due to hydrostatic compressive stress. It is possible to obtain a still more general inequality [5] which also involves the friction in volume change due to deviatoric shear stress, a phenomenon which was termed the inverse friction. Further generalizations of the frictional phenomena, the sufficient stability condition, and the corresponding flow rule are possible by considering frictional phenomena in fracturing stress relaxations, to which we now turn our attention.

2.2   Plastic-Fracturing Theory

Plastic-fracturing theory is a recent extension of classical incremental plasticity [6] which adheres to the use of loading surfaces and flow rule based on these surfaces, and introduces, in addition to plastic strain increments, the fracturing stress relaxations due to micro-fracturing (micro-cracking). The extension to model the inelastic phenomena due to micro-cracking appears to be essential for materials such as concrete as well as rocks. The nature of the theory may be illustrated by Fig. 3, in which plasticity is seen to be characterized by an elastic increment followed by a horizontal plastic strain increment. A material which undergoes only micro-fracturing and no plastic deformation, first studied by Dougill [13,14], is shown in Fig. 3b where the elastic increment is followed by a vertical fracturing stress decrement. While plasticity obviously does not allow strain-softening, i.e., decline of stress at increasing strain, the fracturing theory does. To be able to distinguish strain softening from unloading, the loading surfaces for the fracturing theory must be considered as functions of strains rather than stresses, as was first done by Dougill [13,14], who also introduced the normality rule in the strain space to obtain fracturing stress relaxations. The plastic-fracturing theory is a combination of plastic and fracturing theories and is illustrated in Fig. 3c, where the elastic increment is followed by a horizontal plastic strain increment and then by a vertical fracturing stress decrement. Obviously, the strain softening is also allowed for this theory. The plastic strain increments and fracturing stress decrements are then obtained on the basis of separate loading surfaces in the stress and strain spaces. The characteristic property which allows us to distinguish between plastic and fracturing phenomena is the unloading slope. The plastic phenomena do not lead to any change in the unloading stiffness, while the fracturing phenomena are totally related to a change in the unloading stiffness, and in case of pure fracturing behavior, they preserve total reversibility at complete unloading, as indicated by the fact that the unloading slope in Fig. 3b shoots to the origin. In plastic-fracturing materials (Fig. 3c) the unloading slope decreases but does not point to the origin. If unloading slope is known for each point of the loading diagram, it is possible to uniquely separate the plastic and fracturing effects [see 5].

The plastic-fracturing theory leads to the following incremental stress-strain relations [6]

$$ds_{ij} = 2G\ de_{ij} - 2G\ s_{ij}\ \frac{d\mu}{\tau} - e_{ij}\ \frac{d\varkappa}{\gamma} \tag{6}$$

$$d\sigma = 3K\ d\varepsilon - 2K\beta\ d\mu - \frac{2}{3}\alpha\ d\varkappa \tag{7}$$

in which

$$d\varkappa = H_1 (d\bar\gamma + \alpha' d\epsilon) \tag{8}$$

$$d\mu = H_2 (G s_{km} \, de_{km} + \bar\tau K \beta' d\epsilon_{kk}) \tag{9}$$

Here G = elastic shear modulus, K = elastic bulk modulus (both variable); s_{ij} = deviator of stress tensor σ_{ij}, e_{ij} = deviator of strain tensor ϵ_{ij}, σ = mean stress, ϵ = mean (volumetric) strain = $\epsilon_{kk}/3$; $\mu, \varkappa$ = parameters for plastic and fracturing hardening and softening; $\bar\tau$ = stress intensity, $\bar\gamma$ = strain intensity = $(e_{ij}e_{ij}/2)^{\frac{1}{2}}$; β', α' = plastic and fracturing internal friction coefficients; β, α = plastic and fracturing dilatancy factors giving the ratio of volumetric to deviatoric inelastic increments; and H_1, H_2 = hardening and softening stiffnesses. The inelastic response is here totally characterized by six coefficients, H_1, H_2, β', α', β, α, the dependence of which on the invariants of stress and strain must be determined from experiment. Various other considerations are needed for this purpose and suitable functions for these coefficients have been identified, leading to a rather close agreement with a broad range of experimental data available in the literature [see 6].

In contrast to incremental plasticity, the constitutive equations of plastic-fracturing theory (Eqs. 6-9) involve not only terms which depend on stress (the term with s_{ij} in Eq. 6), but also terms which depend on strains such as the term involving e_{ij} in Eq. 6. These terms appear to be very helpful in representing material behavior in strain-softening regimes, which is due simply to the fact that e_{ij} increases during strain-softening while s_{ij} decreases. These strain-dependent terms give rather different lateral strains and thus allow us to model the large volume dilatancy during strain-softening. Another essential difference from plasticity is that the shear and bulk elastic moduli are variable. As mentioned, their decrease is tied to the growth of fracturing parameter $\varkappa$, for which the following equations were obtained:[2]

$$dG = -\frac{d\varkappa}{2\bar\gamma} \qquad\qquad dK = -\frac{2\alpha}{9}\frac{d\varkappa}{\epsilon} \tag{10}$$

It should be also observed that Eqs. 8, 9 apply only to loading; for unloading modified expressions must be introduced. In analogy to plasticity, one might set $d\varkappa = d\mu = 0$, but then no representation of inelastic behavior on unloading, reloading and cyclic loading would be possible. It is possible, however, to formulate rules which allow for nonzero $d\varkappa$ and $d\mu$ during unloading and cyclic loading [21,5]. These rules consist in the so-called jump-kinematic hardening, in which the center of the loading surface is jumped to the last extreme stress or strain point whenever loading is reversed to unloading or vice versa. Three-way loading-unloading-reloading criteria are needed for this purpose [21,5].

The most important advantage of the plastic-fracturing theory is the fact that the stress-strain relations (Eqs. 6-9) can be brought (for loading) to an incrementally linear form:

$$d\sigma_{ij} = C_{ijkm}(\underset{\sim}{\sigma},\underset{\sim}{\epsilon}) \, de_{km} \tag{11}$$

or $$d\underset{\sim}{\sigma} = \underset{\sim}{C}(\underset{\sim}{\sigma},\underset{\sim}{\epsilon})d\underset{\sim}{\epsilon} \tag{11a}$$

in which C_{ijkm} or $\underset{\sim}{C}$ represent the tensor or matrix of the tangential moduli

---

[2] See [26]

which are functions of the invariants of the stress tensor σ and strain tensor $\underset{\sim}{\epsilon}$; see Ref. 6. The use of tangential moduli is the most effective approach in step-by-step finite element analysis. It must be observed, however, that the matrix of tangential moduli is non-symmetric, which is a consequence of internal friction and is inevitable for close representation of experimental data on the material. This is certainly an inconvenience for numerical finite element analysis. However, it must be emphasized that this type of non-symmetry does not cause material instability as long as the new stability postulate in inequality (2) is satisfied. It should be also noted that tangential moduli C_{ijkm} have a generally anisotropic (non-isotropic and non-orthotropic) form, which is a manifestation of the stress- and strain-induced anisotropy.

The stress-strain relations in Eqs. 6-9 were derived by using loading surfaces that do not involve the third invariants of stress and strain. It is, however, interesting that   the failure envelopes   obtained from these relations (by recording the peaks of the stress-strain diagrams run at various ratios of stress components) have a form that is non-circular on the octahedral plane (π - projection). This is illustrated in Fig. 4, which was constructed from the numerical values of the coefficients of the plastic-fracturing theory from Ref. 6. This shows that the rounded triangular shape of the octahedral section does not necessarily imply the influence of the third stress invariant. This shape can   equally well be caused by the simultaneous influence of stress and strain and the fact that these do not increase proportionally.

The plastic-fracturing theory has been shown to be capable of representing a very broad range of inelastic phenomena, including strain-softening, inelastic dilatancy due to shear and internal friction, as manifested by the great effect of hydrostatic compression in triaxial tests, the increase of volume in pre-peak as well as post-peak deformation, lateral strains, the increase of apparent Poisson's ratio, hysteretic loops during cyclic loading to small as well as high strain levels, etc. [23-25, 28-32].

2.3   Endochronic Theory

The central concept in the endochronic theory, first introduced by Valanis [8] although implied in various preceding works [e.g. 7], is that of intrinsic time, a variable which depends on the length ξ of the path traced by the states of the material in the strain space. A typical definition of intrinsic time, z, is:

$$dz = F_1(z,\underset{\sim}{\sigma},\underset{\sim}{\epsilon})d\xi, \qquad d\xi = \sqrt{\frac{1}{2}\, de_{ij}de_{ij}} \qquad (12)$$

in which F_1 is a function of the stress and strain invariants and models the hardening or softening of the material during the evolution of inelastic strain. The inelastic strain increments are assumed to be proportional to small dz and the constitutive relation of endochronic theory is typified by the following:

$$de_{ij} = \frac{ds_{ij}}{2G} + \frac{s_{ij}}{2G}\, dz \qquad (13)$$

$$d\epsilon = \frac{d\sigma}{3K} + d\lambda \qquad (14)$$

Here an additional variable, $d\lambda$ [9], is introduced to model the inelastic volume dilatancy due to shear. It is also related to intrinsic time:

$$d\lambda = F_2(z, \underset{\sim}{\sigma}, \underset{\sim}{\varepsilon})d\xi \qquad\qquad\qquad (15)$$

It can be shown that the endochronic theory is a special case of viscoplasticity in which the viscosity coefficients depend not only on stress and strain but also on the strain rate [21,7]. The chief advantage of the endochronic theory, first recognized by Valanis is the fact that it is capable of representing the unloading irreversibility, the salient feature of inelastic behavior without the use of any inequalities (unloading criteria). This makes the endochronic theory extremely effective for cyclic loading. Furthermore, the fact that the inelastic strains are tied to one time-like variable dz makes it easy to control the stiffening or softening of the material by changing the rate of growth of the intrinsic time. One aspect which is represented well modeled by the theory is the inelastic volume dilatancy $d\lambda$.

The most significant difference of the endochronic theory from classical plasticity as well as plastic-fracturing theory is the fact that even for loading it can not be reduced to an incrementally linear form given by Eq. 11. Nevertheless, in the vicinity of any specified loading direction the endochronic theory can be linearized and put into this incrementally linear form [21]. However, the tangential moduli C_{ijkm} of this linearized form are not constant and depend on the chosen direction in the vicinity of which the behavior is linearized. It may seem that the lack of incrementally linear formulation would cause significant difficulties in numerical computation. However, finite element programs utilizing endochronic theory have been written [e.g., 10, 11, 12] and no particular convergence difficulties have been encountered.

Endochronic theories have recently been criticized from the viewpoint of material stability and uniqueness of response [19,20]. Subsequently, it was shown however, that the theory can be either modified to satisfy these requirements, for example by the use of jump-kinematic hardening and by unloading-reloading criteria [21,10], or that the strong uniqueness requirements are themselves in question. For example, Rivlin [20] pointed out that when one considers a staircase loading history in the strain space (Fig. 5) and when one lets the size of the stairs shrink to zero and their number go to infinity, the limiting behavior does not approach that for the smooth loading path. It is, however, possible to formulate a refined definition of intrinsic time for which the limit coincides [5], although at the same time the need for doing this may be questioned because the staircase loading path does not cause the same type of damage to the material as does the smooth loading path.

2.4   Further Comments

To exemplify the representation of inelastic behavior that can be obtained with the plastic-fracturing theory, we show some of the fits of test data[3] from Ref. 6 in Figs. 6,7. Just about equally good fits of material behavior have been obtained using the endochronic theory. One might wonder why two rather different theories allow representation of the same phenomena. The answer is that our information on the material behavior is far from complete and is insufficient to completely define the mathematical formulation. Therefore, certain logical assumptions must inevitably be used and the resulting formulation also depends on these. It appears that the most significant difference between various theories of inelastic behavior is obtained when a proportional loading is followed by sudden load increments to the side of the previous loading path; e.g., when an increase of normal stress is followed by a sudden shear stress increment. The different responses for such loading may be graphically illus-
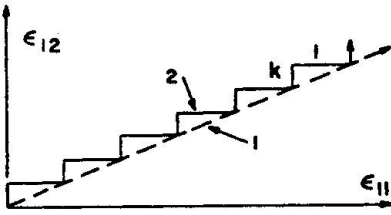

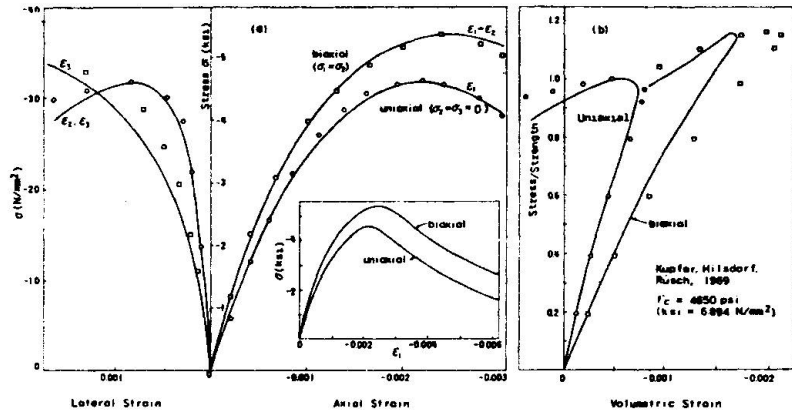[3]See [23-25, 28-32]

Fig. 5 Staircase Loading Path

Fig. 6 Representation of Typical Published Uniaxial and Biaxial Test Data of Plastic-Fracturing Theory [6].
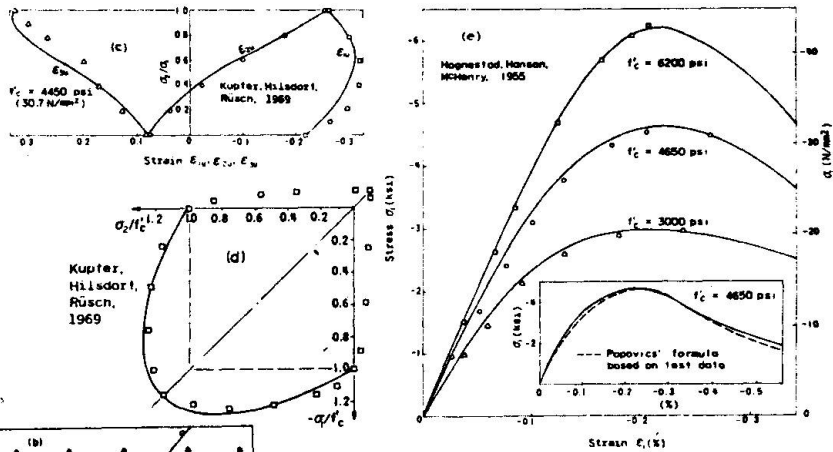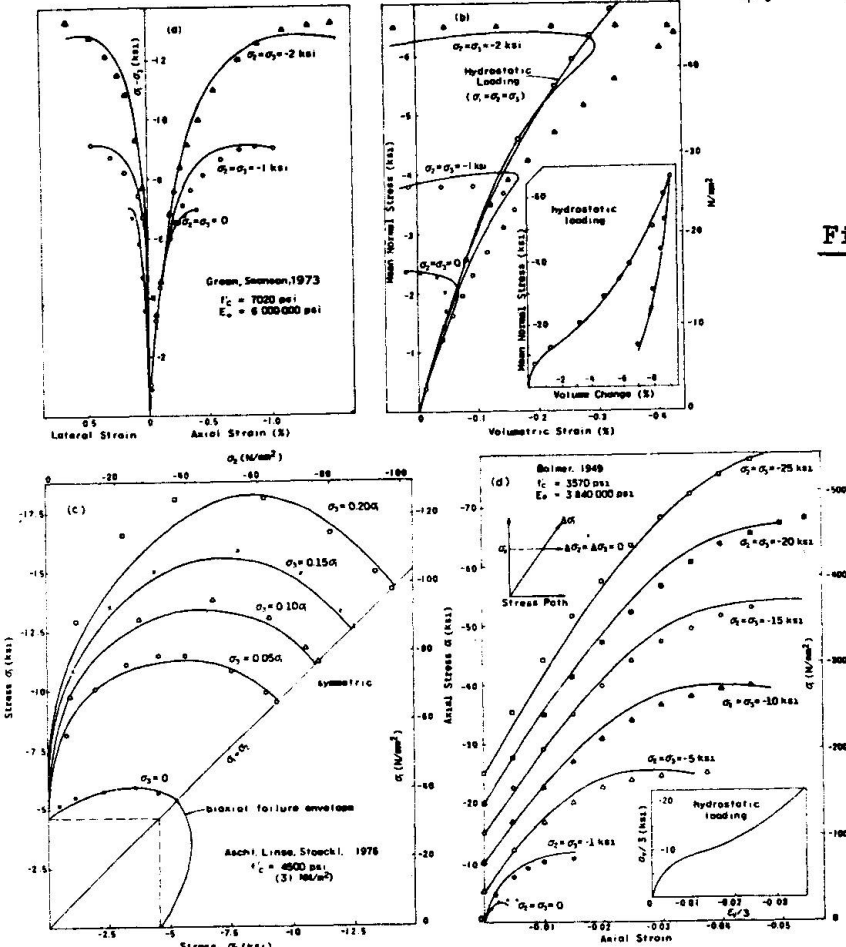
Fig. 7 Representation of Typical Published Triaxial Test Data of Plastic-Fracturing Theory [6]

trated in terms of the inelastic stiffness locus [21]. It is unfortunately for such loading paths that measurements are most difficult and the present experimental information is rather scant. However, improvement of our knowledge for this type of loading is important because the loading "to the side" is characteristic of failures due to material instability.

Many other useful recent models for inelastic behavior of concrete have to be left out. Some of these are distinguished by greater simplicity compared to the models we considered. However, not all of the currently used models are in a correct form. For example, the so-called orthotropic models, in which the increments of strain and stresses are assumed to be related by a tangential moduli matrix of the same form as for an orthotropic material, violate the requirements of tensorial invariance, i.e., invariance of the formulation with regard to rotation of the chosen coordinate axes. [51,52,54]. One obtains with the orthotropic models different results depending on the orientation of the material coordinate axes in the initial state, which is inadmissible. The only way to avoid such spurious non-uniqueness is to rotate the material axes keeping them always oriented in the directions of principal stresses. However, rotation of material axes with regard to the material during the deformation is inadmissible, because it would imply that microcracks and other inelastic defects are rotated against the material. Consequently, the orthotropic models can work correctly only when the directions of principal stresses do not rotate [50], which is, however an unacceptable restriction for finite element programs. It should be observed that these difficulties cannot be detected with the so called true triaxial tests on cubical specimens since the principal stress directions in these tests remain always fixed. We now see that this type of testing has a serious limitation, although it does provide information on the effect of medium principal stress. We need to test the material under conditions of rotating principal stress directions, and further refinement of constitutive theories will have to be based on this type of testing. [50].

The failure conditions have been omitted in our preceding analysis. We take here the point of view that the failure condition for a material with a smooth evolution of response should be an integral part of the constitutive relation. Thus, under stress-controlled conditions the failure is obtained when strains can increase without any change in stress, which corresponds to the peak points of the stress-strain diagram as the failure condition. Under general conditions in which the stresses are not directly controlled the question of failure is more difficult and requires the analysis of stability, both local stability and overall stability of the structure. In such an approach, the stability analysis should in principle also determine ductility. For this purpose, one must analyze the so-called strain-localization instability, which consists in localization of uniformly distributed strain into a narrow band, a phenomenon which borders on fracture. Such analysis of ductility is easy (Figure 8) for a homogeneously stressed specimen, see [17,33], but gets much more difficult in general situations. The principle is not difficult: one must seek the point of singularity of the tangential stiffness matrix of the structure. What makes it difficult, and is normally disregarded in structural analysis, is the fact that there are many possible tangential stiffness matrices to be checked. Even when we consider classical plasticity we have for each finite element two possible stiffness matrices, one for loading and one for unloading. Now, in principle, one would have to check all possible combinations of finite element stiffnesses for loading and unloading from various elements which leads to a preposterously large number of stiffness matrices to be examined. The number of stiffness matrices to be checked gets even larger for theories which allow not just different stiffnesses for loading and unloading, but also for different directions
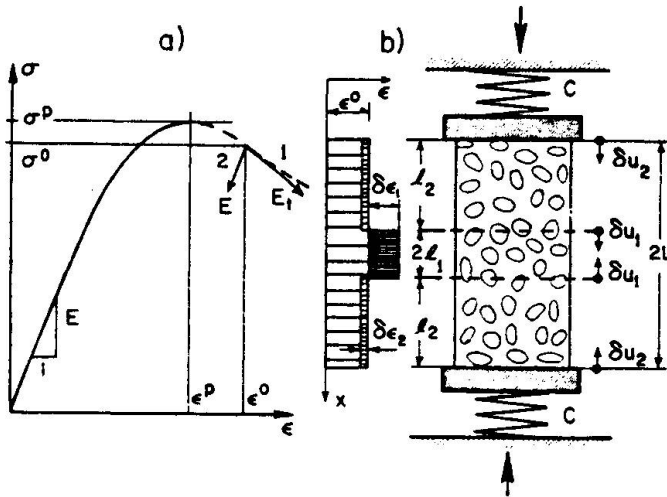
Fig. 8 Simplest Uniaxial Strain-Localization Instability
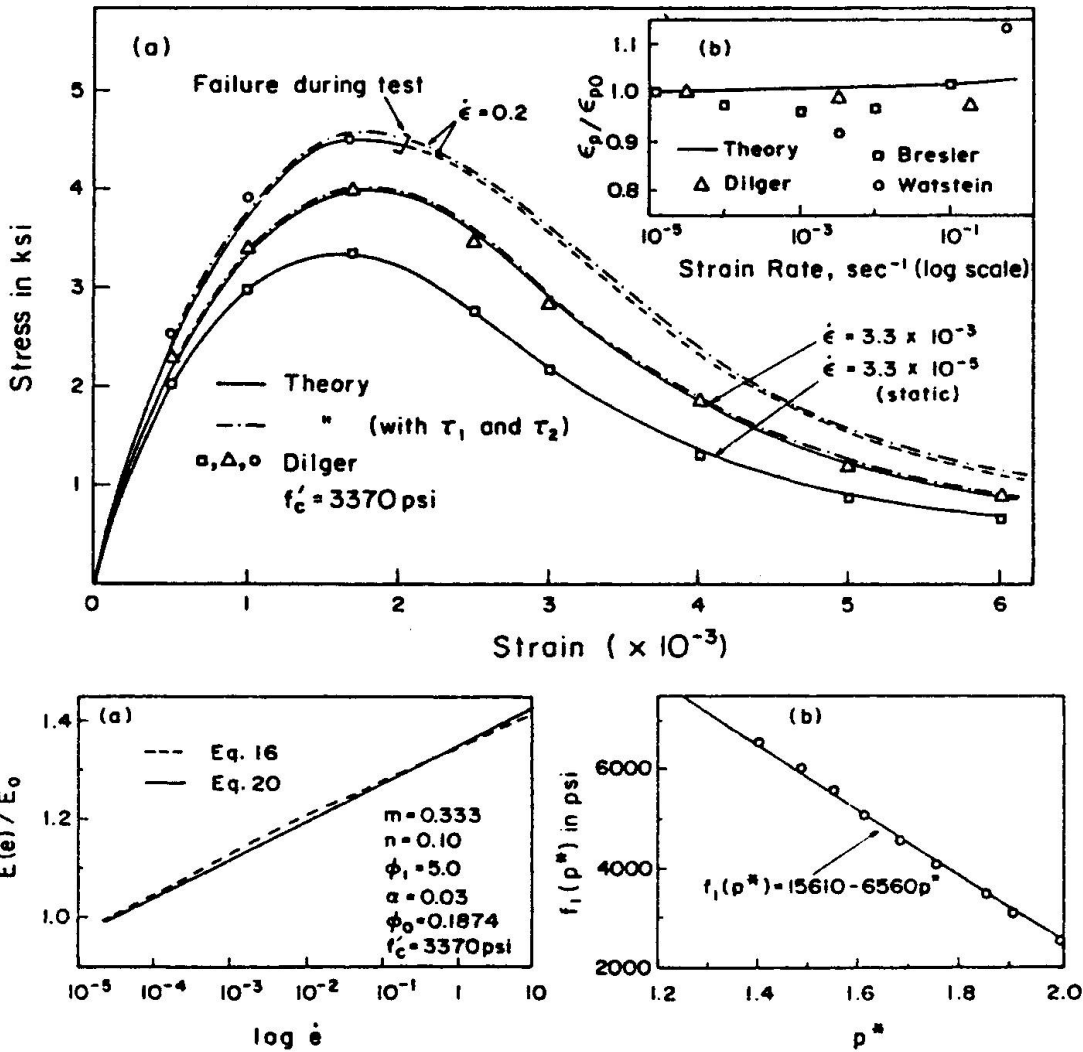due to Strain Softening

Fig. 9 Effect of Strain Rate on Stress-Strain Diagram, Compression
Strength and Elastic Modulus (after [34])

of loading, especially for endochronic theory. For this reason, a different approach, namely that of fracture mechanics is inevitable for the determination of failure under general conditions. We must, however, keep in mind, and this is usually overlooked, that the non-singularity of the incremental stiffness matrix in finite element analysis does not signal stability and lack of failure for the analyst because he normally cannot check (and does not check) all possible incremental stiffness matrices.

3.   SHORT-TIME VISCOELASTIC EFFECTS IN NONLINEAR TRIAXIAL DEFORMATION

3.1.   Strain-Rate Effect

The triaxial constitutive equations are normally formulated on the basis of static loading tests in which failure is usually obtained within several minutes. However, for dynamic structural analysis it is necessary to consider strain rates which differ by several orders of magnitude. The strain rate is known to have a significant effect on the stiffness and strength of concrete and must, therefore, be introduced into the triaxial constitutive relations. We will now briefly outline a recently completed model [34] for the strain-rate effect.

The material parameters for the plastic-fracturing as well as endochronic theory were determined as a function of concrete strength f_c', which appears to be the main parameter affecting the shape of the response curves. Thus, the constitutive relation may be considered in the form:

$$d\sigma_{ij} = C_{ijkm}(\underset{\sim}{\sigma}, \underset{\sim}{\varepsilon}; f_c') d\varepsilon_{km} \tag{16}$$

This equation, for example, models the fact that for a higher concrete strength the uniaxial response curve has a sharper peak and a steeper declining branch. The sharpness of the peak may conveniently   be characterized by the parameter

$$p = \frac{E\varepsilon_p}{\sigma_p} \tag{17}$$

in which σ_p = peak stress and ε_p = strain at peak stress. The static behavior of concrete is to a large extent characterized by the values of elastic modulus E, peak stress (strength) σ_p, and parameter p. Under dynamic loading the values of these parameters are transformed to E^*, σ_p^*, p^*, and one needs to determine how these parameters depend on the strain rate. The strain rate may of course independently affect other parameters of the response, but at present insufficient experimental information on the strain-rate effect in triaxial loading is available for using any more parameters. The foregoing three parameters may be controlled by replacing Eq. 16 with the equation:

$$b \, d\underset{\sim}{\sigma} = \underset{\sim}{C} \left(b \underset{\sim}{\sigma}, a \underset{\sim}{\varepsilon}; f_1(p^*) \right) a \, d\underset{\sim}{\varepsilon} \tag{18}$$

in which

$$b = \frac{f_1(p^*)}{\sigma_p^*}, \qquad a = \frac{E^*}{f_2(p^*)} b \tag{19}$$

Here functions $f_1(p^*)$ and $f_2(p^*)$ characterize the change of peak stress and initial elastic modulus. These functions may be determined by calculating uniaxial response curves from the plastic-fracturing theory equations and

plotting the obtained values of peak stress and elastic modulus against para-
meter p. In this manner, the following relations have been obtained [34]:

$$f_1(p^*) = (15610 - 6560\,p^*)\quad [\text{psi}] \tag{20}$$

$$f_2(p^*) = [0.9 + 0.00006\,f_1(p^*)]57000\,\sqrt{f_1(p^*)}\quad [\text{psi}] \tag{21}$$

in which f_1 and f_2 are in psi.

By analysis of numerous test data on the strain-rate effect, the dependence of
p* and σ_p* on the strain rate was determined[34]:

$$p^* = 2.09 - 0.06\,\log \dot{e} - 0.15\,\sigma_{P_0}\quad (\text{ksi}) \tag{22}$$

$$\sigma_p^* = \sigma_{P_0}(1.4 + 0.09\,\log \dot{e}) \tag{23}$$

in which $\dot{e}$ represents the magnitude of the strain rate. Under triaxial strain
situations this magnitude may be defined as a suitable invariant of the strain
rate tensor, and the expression $\dot{e} = 0.9\,(\dot{e}_{ij}\dot{e}_{ij})^{\frac{1}{2}}$ has been used [34]. The
effect of strain rate on the elastic modulus may be also deduced from the double
power law for concrete creep, the validity of which appears to extend into very
rapid loading. From that approach [48,49], it has been found that [34]

$$\frac{E^*}{E} = \frac{1 + (3.3 \times 10^{-6})^{-n}\varphi_0}{1 + (0.1\,\dot{e})^{-n}\varphi_0} \tag{24}$$

in which φ_0 and n are material constants. Using the foregoing expressions for
p*, E*, σ_p*, f_1 and f_2, the stress-strain relation acquires the form:

$$\dot{\sigma}_{ij} = C_{ijkm}(\underset{\sim}{\sigma},\underset{\sim}{\varepsilon},\dot{e})\,\dot{e}_{km} \tag{25}$$

i.e., the tangential moduli are obtained as functions of not only the stress
and strain invariants but also as functions of strain-rate magnitude $\dot{e}$.

3.2   Strain-Rate Effect with Rapid Creep and Relaxation

Eq. 25 introduces the strain-rate effect in a relatively simple form, but is
incomplete because it can represent neither the increase of strain at constant
stress (rapid creep) nor the decrease of stress at constant strain (rapid re-
laxation). To model all these short-time viscoelastic phenomena, a complete
viscoelastic or visco-plastic formulation is inevitable. As the simplest com-
plete viscoelastic model, one may use the first order differential equation:

$$\dot{\sigma}_{ij} + \frac{1}{\tau_1}\,\sigma_{ij} = C^e_{ijkm}\left(\dot{\varepsilon}_{km} + \frac{1}{\tau_2}\,\varepsilon_{km}\right) \tag{26}$$

in which C^e_{ijkm} are tangential moduli independent of the strain rate, and τ_1,
τ_2 are the relaxation and retardation times. If the tangential moduli were
constant, this equation would correspond to the well-known standard solid. It
is known that the standard solid can describe the viscoelastic properties only
within a relatively narrow range of time delays and time rates, roughly within
one order of their magnitude. To avoid the complexities of using a model with
a broad range of relaxation times, which necessitates higher order differential
equations or integral equations[46], it has been proposed [34] to identify the
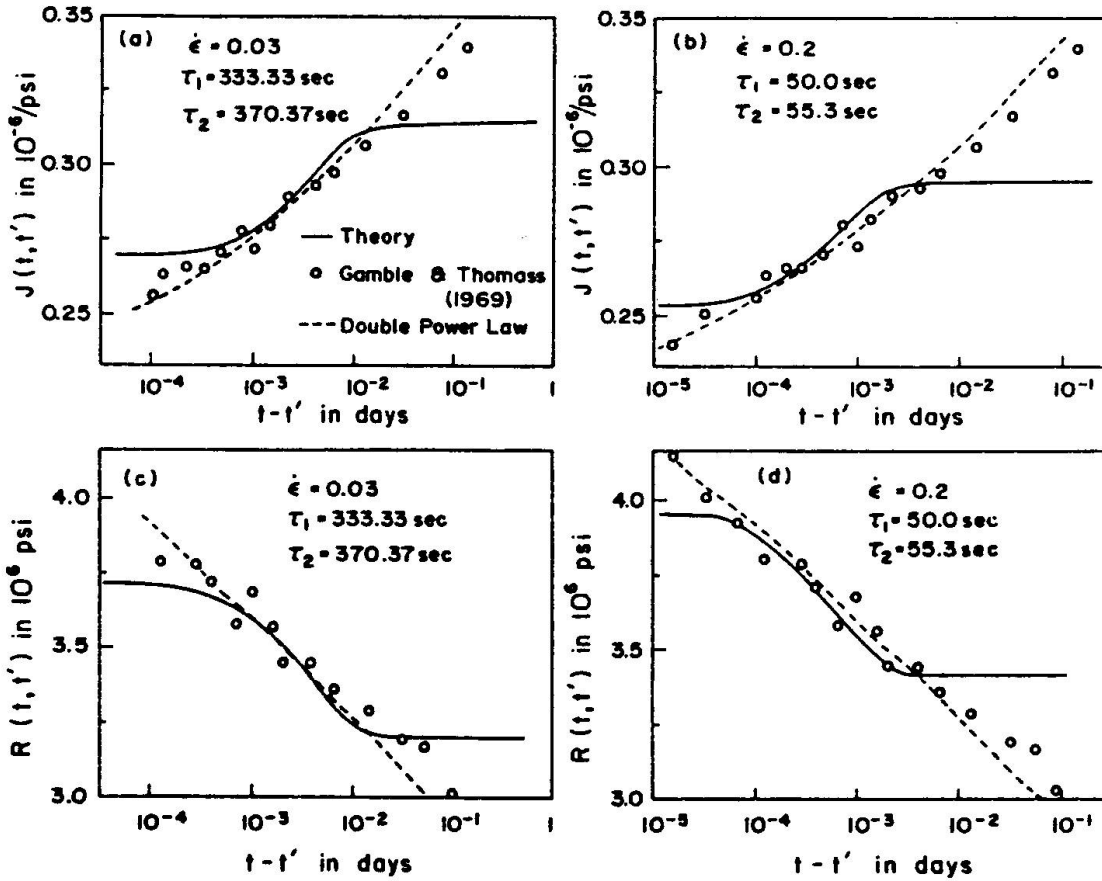
[45]

Fig. 10 Rapid Creep and Rapid Relaxation and Their Theoretical
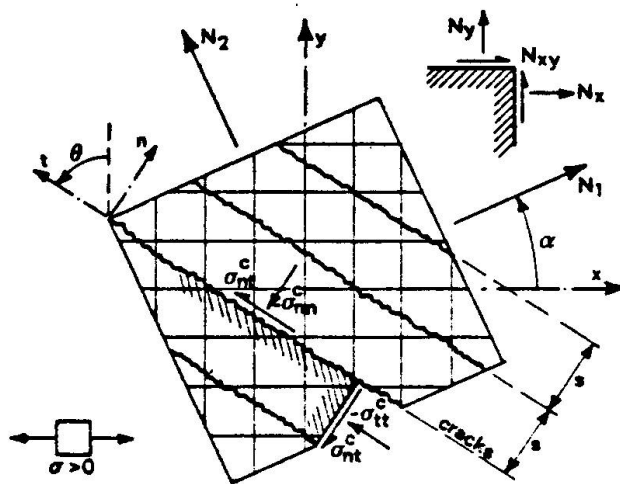Representation from Ref. [34]

Fig. 11 Forces on the Cracks in Reinforced Concrete

parameters in Eq. 26 in such a manner that the response is closely approximated for the strain-rate magnitude $\dot{e}$ that is characteristic of the given dynamic problem, for example, the root-mean-square value $<\dot{e}>$ of strain rate $\dot{e}$ over the time period of interest. One may then determine the parameters in this equation by fitting the corresponding response to various constant strain-rates to that predicted by the previous equation, Eq. 25, so as to obtain optimum approximation near the characteristic strain rate. The necessary calculations have been carried out and it was found that the following parameters give the desired approximation:

$$\tau_1 = (0.1 <\dot{e}>)^{-1} \text{ seconds} \tag{27}$$

$$E_1 = E(\dot{e}) + 1.39 \, k_s \, \frac{dE(\dot{e})}{de} \, \dot{e} \tag{28}$$

$$\tau_2 = \frac{\tau_1 E_1}{2.72 \, E(\dot{e}) - 1.72 \, E_1} \tag{29}$$

$$C^e_{ijkm} = \frac{E_1}{E(<\dot{e}>)} \, C_{ijkm}(\underset{\sim}{\sigma}, \, \underset{\sim}{\varepsilon}, \, <\dot{e}>) \tag{30}$$

With the above parameters, Eq. 26 gives about the same strain-rate effect as Eq. 25, yet at the same time it gives short-time creep and relaxation.

Examples of some comparisons with test data available in the literature, which have been obtained with the foregoing model, are shown in Figs. 9-10 [34].

4. FRACTURED CONCRETE

4.1 Frictional Limit States

The most important characteristics of the surface cracks in concrete are their surface roughness and the interlocking of the pieces of aggregate which accompanies every tangential relative displacement across the crack. It has been customary in finite element analysis to treat aggregate interlock by considering a nonzero shear stiffness of cracked concrete in the direction parallel to the crack, with a value between 0 and its full elastic value. However, this treatment is incomplete and in some situations certainly inadequate. What is important is that any shear stress transmitted across the crack must be accompanied by significant normal compressive stress on the crack. This stress may produce significant tensile stresses in the reinforcement. The simplest way to treat this phenomenon is to consider it as friction, characterized by certain friction coefficient k (typical value 1.4 to 1.7).

A relatively simple and fundamental problem is that of limit states of a concrete panel intersected by parallel cracks and reinforced in arbitrary directions (Fig. 11). This problem has recently been analyzed taking friction into account [53, 68].   This leads to the following limit state envelope (yield criterion)

$$\left[\left(N_x^s - N_x\right) - \beta_1\left(N_y^s - N_y\right)\right]\left[\left(N_y^s - N_y\right) - \beta_1\left(N_x^s - N_x\right)\right] = \left(2\beta_2 N_{xy}\right)^2 \tag{31}$$

(Fig. 12 and 13) in which

$$\beta_1 = \left[\tan\left(\frac{\pi}{4} - \frac{\beta}{2}\right)\right]^2, \quad \beta_2 = \left[2\cos\left(\frac{\pi}{4} - \frac{\beta}{2}\right)\right]^{-2} \tag{32}$$
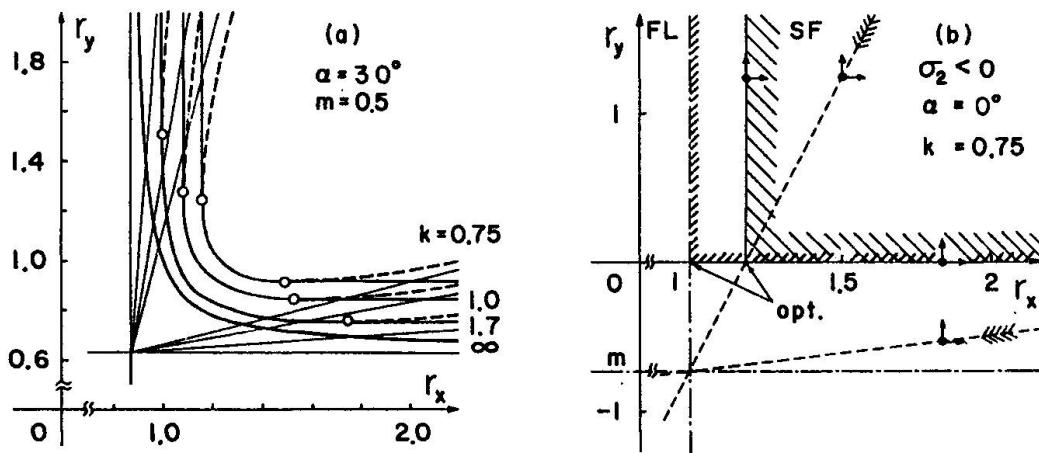
Fig. 12   Example Safe Domain   Envelopes of Reinforcement for Given Load for Various Friction Coefficients k after [54,68](r_x, r_y = reinforcement ratios)
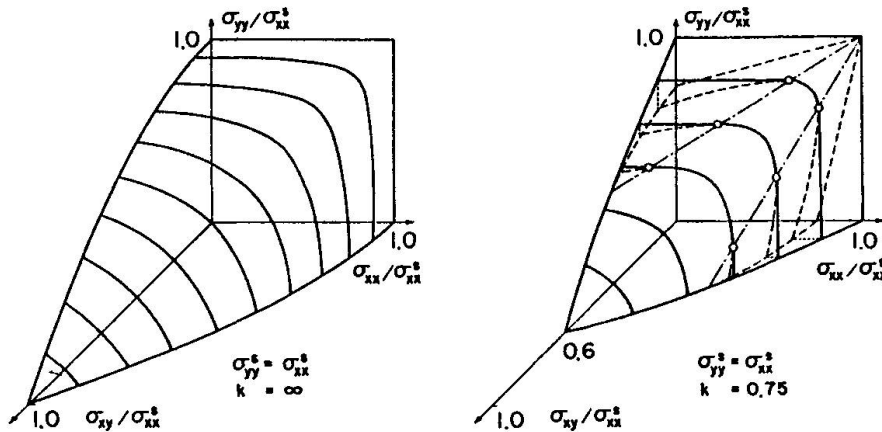
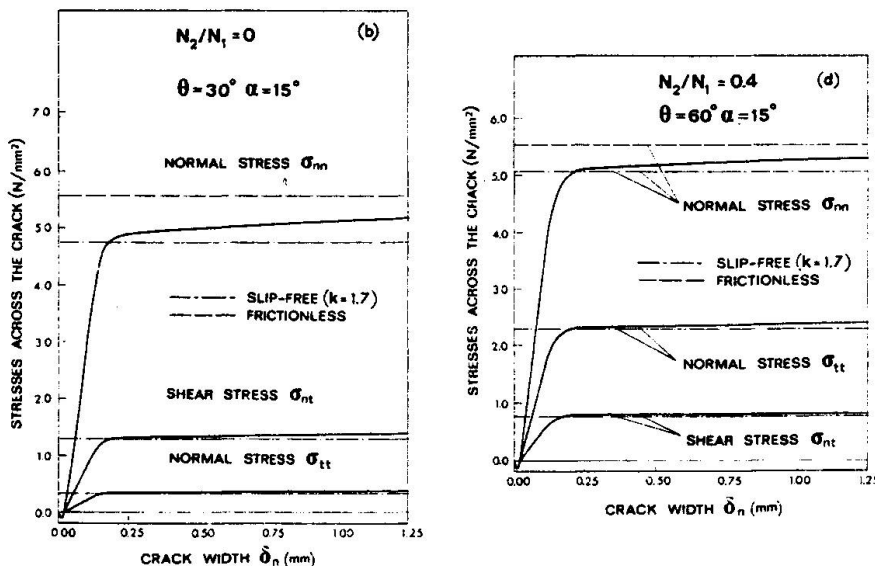**Fig. 13**   Example of Yield Surfaces of Net-Reinforced Panel [54,68]

Fig. 14   Predictions of Experimentally Calibrated Rough Crack Model for Stress vs Crack Width Curves of a Reinforced Panel [67]

where β = friction angle on the cracks; $N_x{}^s$, $N_y{}^s$ = required yield forces in the
reinforcement in the orthogonal x and y directions; N_x, N_y, N_{xy} = components
of the applied internal forces with regard to reinforcement directions. The
classical frictionless solution [55,56] represents a special case of this
equation for $\beta = \beta_1 = \beta_2 = 0$. The solution of frictional and frictionless yield
envelopes and the corresponding yield surfaces are exhibited for a certain
loading situation in Figs. 12-13. It is interesting to observe that the fric-
tional design leads to a heavier reinforcement than does the frictionless design,
which is obtained as a special case when the friction coefficient approaches in-
finity, in which case the normal stress corresponding to a shear stress on the
crack is zero. The differences due to friction are insignificant when the
prinicple directions of applied forces are close to reinforcement directions
but they become rather significant when the reinforcement direction significantly
deviates from the principle direction of applied forces. Thus, we see that the
often stated assumption that the neglect of friction is on the safe side is not
true.

The basic assumption which is considered in the limit design of reinforcement
is that equilibrium with consideration of friction must be achieved for any
direction of cracks in concrete. This assumption differs from that used in
plasticity analysis of reinforced concrete in which no crack direction is
assumed a priori and is determined from the limit state condition itself. From
this fact it may be shown that the frictional limit design with crack of arbi-
trary direction also never yields less reinforcement than the plasticity analysis
(see discussion to Ref. 53).

The frictional limit design with cracks of arbitrary directions has also been
carried out for reinforced plates subject to bending and membrane forces. The
resulting limit state envelopes again, in general, require more reinforcement
than those obtained with the neglect of friction [58].

It must be, however, emphasized that the classical frictionless design approach
leads to reinforcement that is safe in the sense of providing equilibrium for
a given load. However, the frictionless limit state can be developed only after
a very large deformation in which large crack opening is achieved (over 1 cm).
This conclusion has been made on the basis of a much more realistic analysis
utilizing the experimental stress-displacement relation for cracks [67].

4.2   Deformation Due to Rough Cracks

For the analysis of stresses and strains under given loads, one needs the rela-
tionship between the increments of normal and tangential stresses on the crack,
σ_{nn} and σ_{nt}, and the relative normal and tangential displacements across the
crack, δ_n and δ_t. This relationship may be considered in the form:

$$\left\{ \begin{array}{c} d\sigma_{nn} \\ d\sigma_{nt} \end{array} \right\} = \left[\begin{array}{cc} B_{nn} & B_{nt} \\ B_{tn} & B_{tt} \end{array} \right] \left\{ \begin{array}{c} d\delta_n \\ d\delta_t \end{array} \right\} \tag{33}$$

in which B_{nn}, B_{nt}, ... are the stiffness coefficients of the crack. In the sim-
plest approximation one may base this relationship on the concept of frictional
slip with dilatancy, characterized by friction coefficient k and dilatancy ratio
α_d defining the ratio of normal to tangential displacements. If k and α_d are
considered constant, one may deduce the following incremental stiffness matrix
for cracked concrete:

$$
\left\{
\begin{array}{c}
d\sigma_n \\
d\sigma_t \\
d\sigma_{nt}
\end{array}
\right\}
=
\left[
\begin{array}{ccc}
1 & \nu & \pm 2\alpha_d \\
\nu & \dfrac{E_c}{E^*}+\nu^2 & \pm 2\alpha_d \nu \\
\pm k & \pm k\nu & (\pm 2\alpha_d)(\pm k)
\end{array}
\right]
\left\{
\begin{array}{c}
d\epsilon_n \\
d\epsilon_t \\
d\gamma_{nt}
\end{array}
\right\}
\qquad (34)
$$

in which the $\pm$ signs refer to slips of various directions [54]. An interesting aspect of this stiffness matrix is that it is singular, which is the consequence of the friction relation. However, the singularity of this matrix is not a problem in reinforced concrete because the deformation is stabilized by the reinforcement. The stiffness matrix in Eq. 34 has been used also in the analysis of reinforcing nets and again it was found that in general it requires heavier reinforcement than the classical service stress design with frictionless cracks in the principal strain direction [57].

Experimental evidence [59-65], however, reveals that the crack stiffness coefficients are extremely variable depending on the normal and tangential displacements across the crack. For very small openings, the cracks offer a very large resistance to shear displacement while for large crack openings this resistance may become very small. At small crack openings, even a very small tangential displacement across the crack results in very large compressive stresses, while for large crack openings even large tangential displacements do not produce large compression stresses. Algebraic formulas which describe the dependence of stiffness coefficients B_{nn}, B_{nt}, etc. as determined from test results available in the literature were given in Ref. 67. Superimposing the deformations on the cracks to those due to solid concrete between the cracks, one can obtain the flexibility matrix of cracked concrete. For small crack openings this matrix can be written in an explicit form, as follows [67]:

$$
\left\{
\begin{array}{c}
d\epsilon_n \\
d\epsilon_t \\
d\gamma_{nt}
\end{array}
\right\}
=
\left[
\begin{array}{ccc}
D_{11}+A|\sigma_{nt}|^P\sigma_{nn}^{-2}, & D_{12}, & \pm A\,p\,|\sigma_{nt}|\sigma_{nn}^{-1} \\
D_{21} & , D_{22}, & 0 \\
\pm B|\sigma_{nt}|^{P+1}\sigma_{nn}^{-2} & , 0, & D_{33}+B(p+1)|\sigma_{nt}|\sigma_{nn}^{-1}
\end{array}
\right]
\left\{
\begin{array}{c}
d\sigma_n \\
d\sigma_t \\
d\sigma_{nt}
\end{array}
\right\}
$$

$$(35)$$

in which A, B, p = material constants which depend on crack spacing s, and D_{11}, D_{12} ... = flexibility coefficients of solid concrete between the cracks. The $\pm$ sign refers to various directions of shear strain. It is instructive to observe that this matrix contains large off-diagonal terms which determine the normal stress produced by shear strain and the change in shear stress associated with normal strain. Shear stiffness reduction [66] is insufficient [67,54].

For the structural analyst, a natural question is the magnitude of error caused by leaving out the off-diagonal terms or considering them equal to ensure symmetry of the matrix. As explained at the outset, the asymmetry of the stiffness matrix, since it is of frictional type, is not likely to cause instabilities; however, it is inconvenient since most available finite element codes assume symmetric stiffness matrices. This question requires   deeper examination but at this time we can say that there exists cases where for which the neglect of the off-diagonal terms is significant. There may of course exist

numerous other cases where it is not so.

As already mentioned, the rough crack model with crack stiffness coefficients determined directly from measurements can be used to predict the limit states. The results of such calculations [67] are exemplified in Fig. 14.

Consideration of crack friction and dilatancy is likely to be most important in dynamic problems, which are normally characterized by highly non-proportional stress histories. Such stress histories in individual finite elements were, for example, observed in large scale dynamic finite element analysis of nuclear pre-stressed concrete pressure vessels subjected to internal explosive energy re-lease. Fig. 15 shows an example of calculation results from Ref. 69 (these cal-culations did not include crack friction and dilatancy). The fact that the finite elements undergo cracking in multiple directions is an obvious signal of highly non-proportional stress histories.

5.   FRACTURE PROPAGATION

Structural analysis of reinforced concrete necessitates not only the knowledge of the behavior of existing cracks but also of their propagation. For this purpose, it seems preferable to model this phenomenon in terms of element-wide blunt smeared crack band rather than a single sharp interelement crack. This corresponds to the observed fact that cracks in concrete tend to be diffuse and spread over a large zone, especially at the front of propagation. At the same time, the concept of an element-wide blunt smeared crack band is much more con-venient than interelement sharp cracks, particularly when the fracture propagates in an unknown and arbitrary direction, proceeding in a skew path through the mesh. Compared to the use of sharp interelement cracks, it is not necessary to split each node in two when the crack advances, and this avoids the need for node renumbering and changes in topological connectivity of the mesh with the neces-sary recalculations of the structural stiffness matrix. Moreover, when the crack direction is unknown it is not necessary to vary the direction of the in-terface between two finite elements and move the location of the node into which the crack is about to advance. It suffices to modify the stiffness of the ma-trix of the finite elements that undergo cracking, setting the normal stiffness in the direction across the cracks equal to zero.

The propagation of smeared crack bands in finite element meshes has so far been determined on the basis of the stress value compared to the strength limit [70, 73]. It has, however, been demonstrated that this approach can give widely different results depending on the choice of the finite element mesh, and is, therefore, unobjective [74-77]. As the size of the finite elements in the region of the crack front is reduced to zero, the crack band tends to localize into a single element strip, and since the stress in the stress in the element in front of the crack band tends to infinity, the load which causes further extension of the crack band is always found to approach zero when the mesh refinement is con-sidered.

5.1   Energy Criterion for Crack Band Propagation

A propagation criterion that is independent of the mesh size is the rate of the energy release per unit length (or in three-dimensions, unit area) of the crack band. This is the same concept as in fracture mechanics of sharp cracks [78]. In a finite element scheme, the energy release rate, G, may be approximated as $\Delta U/\Delta a$, where ΔU is the energy release of the structure as the crack band advances the length Δa of a single finite element. If the value of $G = - \Delta U/\Delta a$ is less
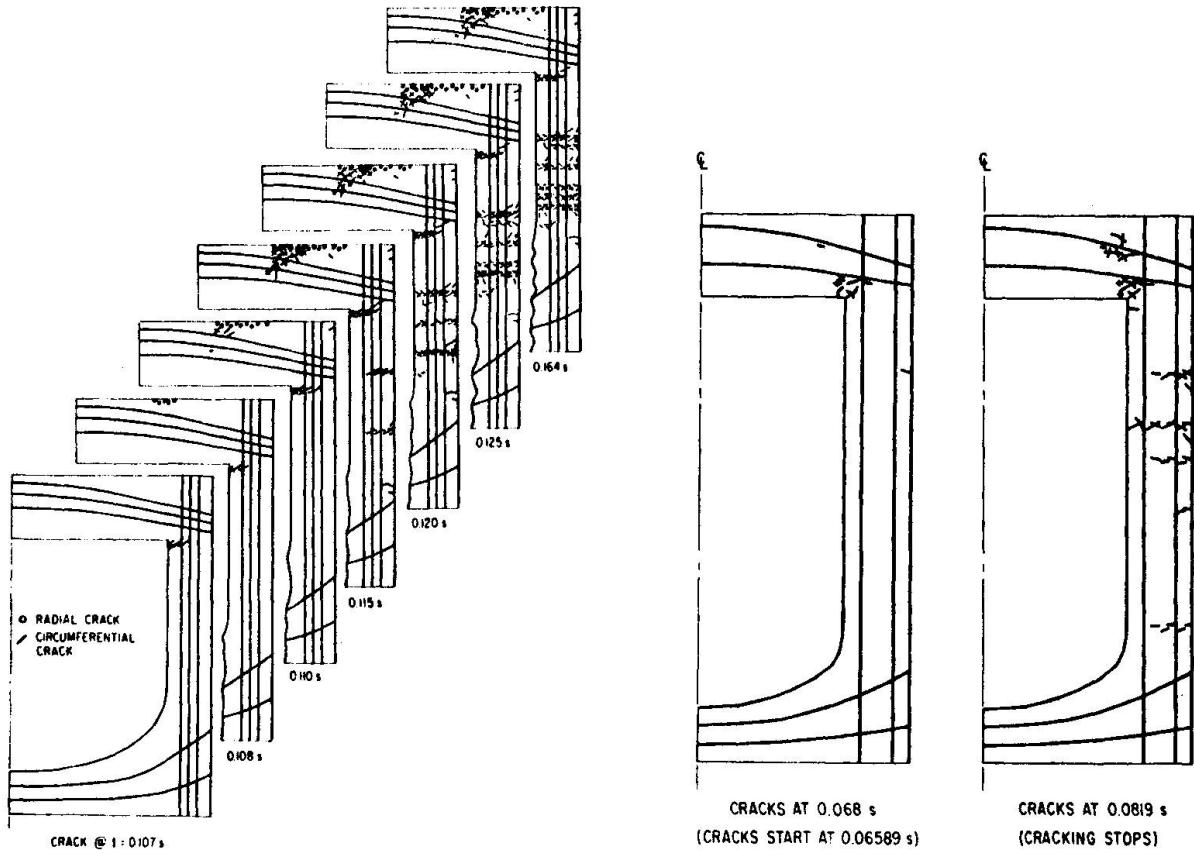
Fig. 15   Example of Cracking Sequence in Dynamic Loading of Concrete
Reactor Vessel, Calculated by Finite Elements [69] (Left:
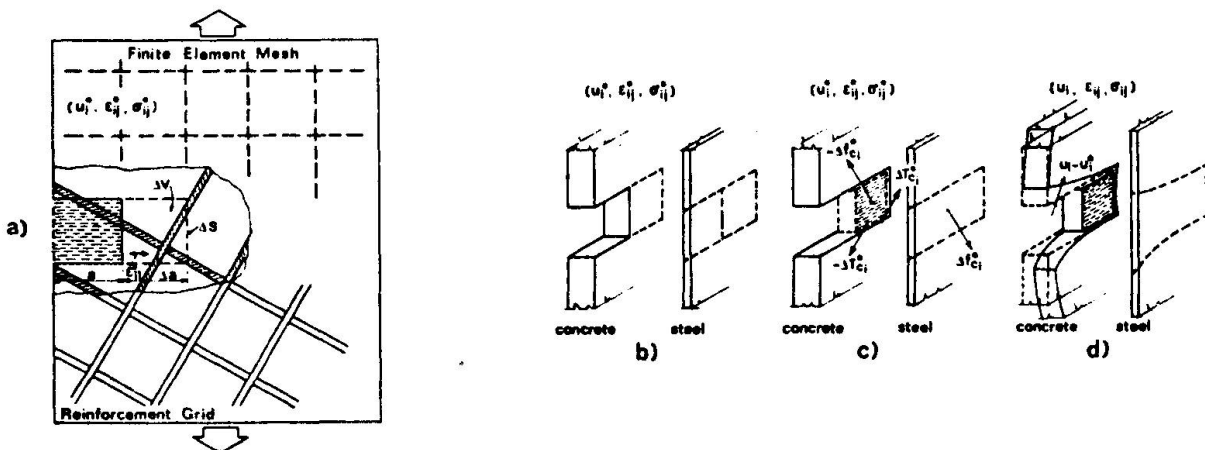Pool-Type vessel, Right: Loop-Type Vessel for LMFBR)

Fig. 16   Crack Band Advance in Finite Element Mesh

than a certain critical energy release rate, G_{cr}, the crack band cannot propagate. If G attains the critical value G_{cr}, the crack band is extended into the next finite element.

The calculation of the energy release, ΔU, may be carried out similarly to Rice's formula for the extension of the notch in an elastic material [78]. The only generalization necessary is to take into account the fact that, in contrast to a notch extension, the material is not removed but merely penetrated by parallel cracks, causing that only part of the energy stored in the material is lost by the crack band extension [75]. A second generalization necessary for reinforced concrete is to take into account the effect of reinforcing bars crossing the finite element into which the cracks propagate [76].

The change of the potential energy of an elastic body due to the extension of the crack band into a volume ΔV of the element in front of the crack band is independent from the history in which this extension happens and may, therefore, be separated into two stages:

Stage I. - Volume ΔV of the element ahead of the crack band gets intersected by cracks in the direction of the principal tensile stress (Fig. 16). At the same time, the stress and deformation state in the rest of the body is imagined to remain fixed (frozen). Accordingly, one must introduce surface tractions ΔT^o_{ci} acting on the boundary ΔS of volume ΔV, and in case of reinforced concrete, also forces Δf^o_{ci} transmitted from steel into concrete within volume ΔV. These tractions and forces are calculated so as to replace the previous action of the volume ΔV of the concrete upon the rest of the body (Fig. 16c).

Stage II. - Forces ΔT^o_{ci} and Δf^o_{ci} are then released by gradually applying the opposite forces $-\Delta T^o_{ci}$ and $-\Delta f^o_{ci}$ (Fig. 16).

The energy changes corresponding to these two stages may be expressed as

$$\Delta W_{(\Delta V)} = - \int_{\Delta V} \frac{1}{2} \left(\sigma^{c^o}_{ij} e^o_{ij} - E'_c e^{o^2}_{11} \right) dV \tag{36}$$

$$\Delta L = \int_{\Delta S} \frac{1}{2} \Delta T^o_{c_i} \left(u_i - u^o_i \right) dS + \int_{\Delta V} \frac{1}{2} \Delta f^o_{c_i} \left(u_i - u^o_i \right) dV \tag{37}$$

and the total energy release associated with the single element advance of the crack band is

$$\Delta U = \Delta W_{(\Delta V)} + \Delta L \tag{38}$$

Here, u_i = displacements in cartesian coordinates x_i ($i = 1,2,3$), σ_{ij} = cartesian stress components, e_{ij} = cartesian components of the small strain tensor, superscript c refers to concrete, u^o_i, e^o_{ij}, and σ^c_{ij} = values of displacements, strains and stresses in volume ΔV before the advance of the crack band (before Stage I); $E'_c = E_c$ for plain stress and $E'_c = E_c/(1 - v^2_c)$ for plain strain, in which E_c = Young's modulus for plain concrete and v_c = Poisson's ratio.

The foregoing equations constitute the basic energy relations for the propagation of crack bands in reinforced concrete. These equations apply only for linearly elastic behavior outside   the crack band. It is, however, possible

[76] to generalize the expression for ΔU for the case of nonlinear behavior of concrete outside the crack band and for the yielding of steel. To this end, the coefficients 1/2 in the expression for ΔU must be replaced by integrations over the deformation path of Stage II. In case of nonlinear behavior an additional restriction must be imposed; namely, the width w of the element-wide crack band either must coincide with the actual crack band width w_c for the material or one must use a path-independent integral such as the J integral instead of Eq. 37. This is necessary because the nonlinear behavior also causes a loss of energy which must be distinguished from the loss of energy due to fracture extension.

5.2 Effect of Bond-Slip of Reinforcement

In finite element analysis of reinforced concrete it has been customary to assume that the steel bars are rigidly attached to concrete at the nodes. This treatment is, however, not only physically unjustified but also unobjective and leads to incorrect convergence. The bars connecting the nodes on the opposite sides of the crack band represent an elastic connection, the stiffness of which is inversely proportional to the distance between the nodes, i.e., to the width w of the crack band. Thus, as the width of the crack band tends to zero, the stiffness of the connection across the crack band increases to infinity, which in the limit prevents any opening of the crack band. So it is clear that no cracking can be obtained in the limit. Moreover, one can check that significant differences of the results are caused by the lack of bond-slip than when meshes of various practically possible sizes are considered [75-77].

To obtain an objective and properly convergent formulation, one must take into account the bond-slip. The bond-slip in reality occurs over a certain length, L_s (Fig. 17). The most realistic treatment of the bond-slip would call for using separate nodes for concrete and steel connected by some nonlinear linkage elements representing forces transmitted by bond. However, this approach would be quite cumbersome. In the spirit of the approximations involved in the smeared crack band model, it should be sufficient to introduce the bond slip in such a way that the stiffness of the connection provided by the steel bars crossing the crack band would be roughly correct and independent of the mesh size.

So, for the sake of simplicity, the actual curvilinear variation of the bond forces and the axial forces in the bars (Fig. 17) may be replaced by an idealized piece-wise variation of the bond force and the corresponding piece-wise linear variation of the actual axial force in the bars. The latter may further be replaced by a piece-wise constant variation of the axial force, such that the overall extension of the bar over the distance of the bond-slip be roughly the same. The actual distance of the bond slip may be approximated as

$$L_s = \frac{(\sigma_s - \sigma_s')A_b}{U_b'} \tag{39}$$

in which A_b = cross-sectional area of the steel bar; σ_s = tensile stress in the bar at the point it crosses the crack band; σ_s' = tensile stress in the bar at the end of the slipping segment, i.e., at locations sufficiently remote from the crack band; and U_b' = the ultimate bond force as determined from pull-out tests. Certain reasonable estimates of σ_s and σ_s' can be made on the basis of the yield stress of steel and the tensile strengths of concrete [76].

Expression (39) gives the actual bond-slip length as a fixed property charac-
teristic of the steel-concrete composite. For the purpose of finite element
analysis, the actual bond-slip length L_s may be replaced by some modified
length L_s^* (Fig. 17f) such that the steel stress over this length is uniform
and the slip of steel bar within concrete may be considered as free. The length
L_s^* is determined from the condition that the extension of the steel bar over
the length L_s be the same, as already stated. In this manner, the following
expression for the equivalent free bond-slip length can be obtained [72]:

$$L_s^* = \frac{L_s}{2} \frac{p^*}{p(1 + pn - p^*n)} + k_b \frac{w}{2}$$ (40)

Here w represents the width of the element-wide crack band, k_b is a correction
factor smaller than 1.0 but close to 1.0 (for which also a theoretical expres-
sion exists)[72], p is the reinforcement ratio (the ratio of the cross-section
areas of reinforcement and concrete), n is the ratio of Young's modulus of
steel to that of concrete, and p^* is a certain modified reinforcement ratio
which may be conveniently chosen so as to make the length L_s^* equal to the dis-
tance between the adjacent nodes located across the crack band ($L_s^!$ in Fig. 17h).

5.3   Typical Numerical Results

Some typical numerical finite element results [76] are plotted in Fig. 17. Con-
sidered is a rectangular reinforced concrete panel subjected to tensile forces
at two opposite ends. A symmetric centrally located crack band normal to the
applied loads is assumed to grow from the center of the panel symmetrically
towards its sides. Using the energy criterion and the free bond-slip length,
one can calculate the multiplier α of the applied loads that is necessary to
cause the extension of the crack band of length a; see [76]. As expected, mul-
tiplier α decreases as the crack band length a increases. Computations have
been carried out [76] for three different rectangular meshes, the sides of which
are in the ratio 4:2:1, labeled as A, B, C (Fig. 17 i). The grid used in the
calculations was a uniform square grid and each square element was assumed to
consist of two constant strain triangles. Both triangular elements forming one
square were assumed to always crack simultaneously.

It may now be observed in Fig. 17 i that the results for the three different
meshes fall approximately on the same curve. It has been previously demonstra-
ted [75] that in case of the classical strength criterion, the results of the
calculation for these three meshes are widely different and deviate from each
other as much as 100%. It is also noteworthy that coincidence of the results
is obtained for plain concrete (p=0) as well as for reinforced concrete(p >0).
It has been also previously shown [72] that the results for reinforced concrete
for these three meshes are far apart when the strength criterion is used, and
also when the energy criterion without the bond slip of steel is considered.

The results presented in Fig. 17 i and numerous further results given in [75,76]
demonstrate that the proposed method is objective, i.e., independent of the
chosen finite element mesh.

The solid curves indicated in Fig. 17 i represent the exact solutions for a
sharp crack according to linear fracture mechanics. From this comparison it is
seen that the concept of an element-wide crack band may be also used as a con-
venient and effective approximation to the propagation of sharp cracks, gaining
all the practical computational advantages of the blunt smeared crack band model
as compared to considering sharp inter-element cracks. One may now naturally

ask: What is then the physical difference between the smeared crack band and the sharp inter-element crack?

Obviously, up to a certain rather wide crack band the difference is insignificant in these computations. For finer meshes, the real difference arises only through the value of the energy-release rate that is to be considered in the calculation. In an on-going work that has not yet been completed, it is found that the critical energy release rate for a smeared crack band cannot be considered to be a fixed material property (unless the width of the band tends to zero), and must be regarded as a function of the band width as well as of the rate of change of G and of the stiffness of the structure surrounding the front of the crack band. When the differences in the critical energy release rate between a smeared crack band and a sharp crack are considered, the results of computations cannot be, of course, identical. It is by means of the variation of the critical energy release rate that one can explain deviations from fracture mechanics predictions as observed on concrete specimens the size of which is not sufficiently large compared to the aggregate size [82,79-81].

5.4   Equivalent Strength Criterion

Determination of the energy release ΔU needed for the propagation criterion requires two finite element calculations, one for the initial crack band length and one for the crack band extended by one element. It has been found [75,76] that calculations may be simplified by approximately estimating the energy release rate on the basis of the stress state in the uncracked finite element just in front of the crack band. The energy release rate becomes (approximately) critical when the normal stress orthogonal to the crack direction attains the value

$$(\sigma_{22}^0)_{cr} = \sigma_{eq} = c \sqrt{\frac{E_c' \, G_{cr}}{w}} \tag{41}$$

in which σ_{eq} was named the equivalent strength, and c is a coefficient characteristic of the given element type. Generally, c is close to 1.0. For a square element consisting of four linear strain triangles, c = 0.826 [77] while for a square element consisting of only two constant strain triangles c = 0.921 [75,76]. It is interesting to observe that σ_{eq} increases as the width of the crack band decreases, and tends to infinity as the element size approaches zero. Obviously, the equivalent strength criterion in Eq. (41) must give results that significantly differ from those for a constant strength limit. In a work still in progress, it has been found that the equivalent strength criterion, which is in Eq. (41) given only for plain concrete, may be extended to reinforced concrete. For this purpose, a corrective term which involves a reinforcement ratio must be added to the expression in Eq. 41.

5.5   Basic Results

The research results just outlined lead to several important conclusions: (1) The use of a constant strength limit for determining extension of a crack band in a finite element mesh is unobjective and has incorrect convergence behavior. The results may differ by as much as 100% when meshes of different size are used. (2) An objective and physically realistic criterion for crack band extension must be expressed in terms of the energy release rate by unit length of the crack band. Expressions for calculating the energy release rate in a finite element program have been formulated. (3) To achieve an objective and properly convergent propagation criterion for reinforced concrete, the bond-slip between steel reinforcement and concrete must be taken into account. This may be conveniently done in terms of the equivalent free bond-slip length, for which a
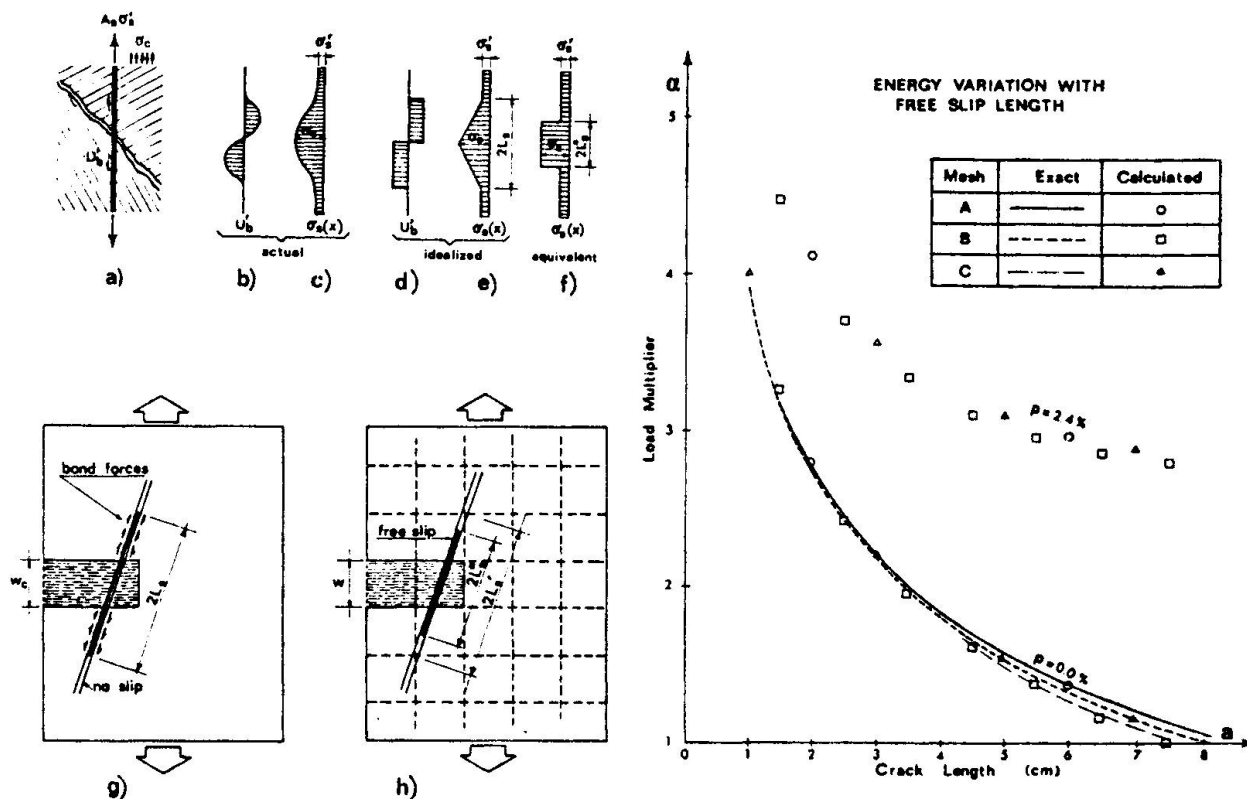
Fig. 17 Effect of Bond Slip and Some Typical Numerical Results [76]

simple approximation exists. (4) As an acceptable approximation, the energy criterion may be replaced by an equivalent strength criterion such that the strength limit depends on the width of the element-wise smeared crack band.

6. CONCLUDING REMARKS

One major impression which may result from this exposition is that the advanced theories of the mechanical behavior of concrete are not, in the most part, very simple. This fact is certainly unappealing to a structural analyst, and it would be outright objectionable to a physicist who knows that the true form of the laws of nature is simple, not complicated. We must recognize, however, that we don't move here in the world of a physicist whose mind is occupied only with the fundamental laws describing individual physical phenomena. The response of heterogeneous composite such as concrete is influenced by numerous physical phenomena and processes intervening simultaneously. Realizing this, it should not be altogether surprising to us that we have been unable so far to describe the complicated response of concrete by a few simple laws. We must certainly strive hard for such an outcome, but at best we probably achieve it only to a limited extent. Fortunately, we are blessed with powerful tools, the electronic computers, which can handle even rather complicated mathematical models. It is due to this fortunate situation that our effort to develop more accurate, realistic and refined mathematical models of concrete should bear fruit.

7. ACKNOWLEDGMENT

8.   REFERENCES

1.   Drucker, D.C., "Some Implications of Work Hardening and Ideal Plasticity,"
       Quarterly of Applied Math., Vol. 7, 1950, pp. 411-418.

2.   Drucker, D.C., "A Definition of Stable Inelastic Material," J. Appl. Mech.,
       Trans. ASME, Vol. 26, 1959, pp. 101-106.

3.   Fung, Y.C., "Foundations of Solid Mechanics," Prentice Hall, Englewood
       Cliffs, N.J., 1975 (Chapter 6).

4.   Malvern, L.E., "Introduction to the Mechanics of a Continuous Medium,"
       Prentice-Hall, Englewood Cliffs, N.J., 1969.

5.   Bažant, Z.P., "Work Inequalities for Plastic-Fracturing Materials," Intern.
       J. of Solids and Structures, Vol. 16, 1980.

6.   Bažant, Z.P., Kim, S.S., "Plastic-Fracturing Theory for Concrete," J. of
       the Engng. Mech. Div., Proc. Am. Soc. of Civil. Engrs., Vol. 105, June
       1979, pp. 407-428, with Errata in Vol. 106 (also as Preprint 3431, ASCE
       Annual Convention, Chicago, Oct. 1978).

7.   Schapery, R.A., "On a Thermodynamic Constitutive Theory and Its Applica-
       tions to Various Nonlinear Materials," Proc. IUTAM Symp. East Kilbride,
       June 1968, ed. B.A. Boley, Springer Verlag, New York, 1968.

8.   Valanis, K.C., "A Theory of Viscoplasticity without a Yield Surface,"
       Archiwum Mechaniki Stossowanej (Archives of Mechanics, Warsaw), Vol. 23,
       1971, pp. 517-551.

9.   Bažant, Z.P., Bhat, P., "Endochronic Theory of Inelasticity and Failure
       of Concrete," J. of the Engrg. Mech. Div., Proc. Am. Soc. of Civil Engrs.,
       Vol. 102, 1976, pp. 701-722.

10.   Bažant, Z.P., Shieh, C.L., "Total Strain Theory and Path-Dependence of
       Concrete," J. of the Engng. Mech. Div., Proc. ASCE, Vol. 106, Oct. 1980
       pp.

11.   Sørensen, S.I., Arnesen, A., Bergan, P.G., "Nonlinear Finite Element
       Analysis of Reinforced Concrete Using Endochronic Theory," Finite Elements
       in Nonlinear Mechanics (Proc. of Int. Conf. held at Geilo, Norway, 1977)
       Tapir, Norwegian Inst. of Tech. Trondheim, Vol. 1, pp. 167-190, 1978.

12.   de Villiers, I.P., "Implementation of Endochronic Theory for Analysis of
       Concrete Structure," Ph.D. Dissertation, University of California,Berkeley
       1977.

13.   Dougill, J.W., "On Stable Progressively Fracturing Solids," ZAMP (Zeitschrift
       für Angewandte Mathematik und Physik), Vol. 27, Fasc. 4, 1976, pp. 423-437.

14.   Dougill, J.W., "Some Remarks on Path Independence in the Small in Plasti-
       city," Quarterly of Appl. Math., Vol. 32, 1975, pp. 233-243.

15.   Mandel, J.,"Conditions de Stabilité et Postulat de Drucker," in Rheology
       and Soil Mechanics," IUTAM Symp. held in Grenoble in 1964, ed. by J.
       Kravtchenko and P.M. Sirieys, Springer Verlag, Berlin, 1966, pp. 58-68.

16.   Maier G., "Incremental Plastic Analysis in the Presence of Large Displace-
       ments and Physical Stabilizing Effects," Int. J. of Solids and Structures,
       Vol. 1, 1971, pp. 345-372.

17. Bažant, Z.P., "Instability, Ductility and Size Effect in Strain-Softening Concrete", J. of the Engineering Mechanics Division, Proc. ASCE, Vol. 102, April 1976, EM2, pp. 331-344.

18. Hill, R., Rice, J.R., "Elastic Potentials and the Structure of Inelastic Constitutive Laws," SIAM J. of Appl. Math., Vol. 25, No. 3, 1973 pp. 448-461.

19. Sandler, I.S., "On the Uniqueness and Stability of Endochronic Theories of Material Behavior," Trans. ASME, Series E, Journal of Applied Mechanics, Vol. 45, 1978, pp. 263-266.

20. Rivlin, R.S., "Some Comments on the Endochronic Theory of Plasticity," Report No. CAM-100-33, Center for the Application of Math., Lehigh Univ., Bethlehem, 1979; to appear in Int. J. of Solids and Structures.

21. Bažant, Z.P., "Endochronic Inelasticity and Incremental Plasticity," Int. J. of Solids and Structures, Vol. 14, 1978, pp. 691-714.

22. Bažant, Z.P., Bhat, P., "Endochronic Theory of Inelasticity and Failure of Concrete," J. of the Engrg Mech. Div., ASCE, Vol. 102, No. EM4, Proc. Paper 12360, April 1976, pp. 701-722.

23. Aschl, H., Linse, D., Stoeckl, S., "Strength and Stress-Strain Behavior of Concrete under Multiaxial Compression and Tension Loading," Technical Report, Technical University, Munich, Germany, Aug. 1976.

24. Balmer, G.G., "Shearing Strength of Concrete under High Triaxial Stress-Computation of Mohr's Envelope as a Curve," Structural Research Laboratory Report No. SP-23, Structural Research Laboratory, Denver, Colo. Oct. 1949.

25. Bresler, B., Pister, K.S., "Strength of Concrete under Combined Stresses," American Concrete Inst. Journal, Vol. 551, Sept. 1958, pp. 321-345.

26. Budiansky, B., O'Connell, R.J., "Elastic Moduli of Cracked Solids," Int. J. of Solids and Structures, Vol. 12, 1976, pp. 81-97.

27. Drucker, D.C. and Prager, W., "Soil Mechanics and Plastic Analysis or Limit Design," Quarterly of Appl. Math., Vol. 10, 1952, pp. 157-165.

28. Hobbs, D.W., "Strength and Deformation Properties of Plain Concrete Subject to Combined Stresses, Part 3: Results Obtained on a Range of Flint Gravel Aggregate Concrete," Technical Report, Cement and Concrete Association, London, England, July 1974.

29. Kupfer, H.B., Hilsdorf, H.K., Rüsch, H., "Behavior of Concrete under Bi-axial Stresses," American Concrete Inst. Journal, Vol. 66, 1969, pp. 656-666.

30. Liu, T.C.Y., Nilson, A.H. and Slate, F.O., "Biaxial Stress-Strain Relations for Concrete," J. of the Struct. Div., ASCE, Vol. 98, No. ST5, Proc. paper 8905, May, 1972, pp. 1025-1034.

31. Popovics, S., "A Numerical Approach to the Complete Stress-Strain Curves of Concrete," Cement and Concrete Research, Vol. 3, No. 5, Sept. 1973, pp. 583-599.

32. Shah, S.P., Chandra, S., "Critical Stress, Volume Change and Microcracking of Concrete," American Concrete Inst. Journal, Vol. 65, No. 9, Sept. 1968, pp. 770-781.

33   Bažant, Z.P., Panula, L., "Statistical Stability Effects in Concrete Strength and Ductility," J. of the Engng. Mech. Div. Proc., ASCE, Vol. 104, 1978, pp. 1195-1212.

34.   Bažant, Z.P., Oh, Byung H., "Strain-Rate Effect in Rapid Nonlinear Triaxial Deformation of Concrete," Structural Engineering Report No. 80-7/640s, Northwestern University, July 1980.

35.   Abrams, D.A., "Effect of Rate of Application of Load on the Compressive Strength of Concrete," Proc. ASTM, Volume 17, Part II, pp. 364.

36.   Atchley, B.L., Furr, H.L., "Strength and Energy Absorption Capabilities of Plain Concrete Under Dynamic and Static Loadings," American Concrete Inst. Journal, Volume 64, No. 11, Nov. 1967, pp. 745-756.

37.   Bresler, B., Bertero, V.V., "Influence of High Strain Rate and Cyclic Loading on Behavior of Unconfined and Confined Concrete in Compression," Report, Division of Structural Engineering and-Structural Mechanics, University of California, Berkeley, California, 1979.

38.   Dilger, W.H., Kock, R., and Kowalczyk, R., "Ductility of Plain and Confined Concrete under Different Strain Rates," presented at ACI Meeting, Houston, Nov. 1978, ACI Special Publication - to appear.

39.   Hatano, T., Tsutsumi, H., "Dynamic Compressive Deformation and Failure of Concrete under Earthquake Load," Proc. of the 2nd World Conference on Earthquake Engineering, Science Council of Japan, Tokyo, 1960. Volume IV, pp. 1963-1978.

40.   Mainstron, R.J., "Properties of Materials at High Rates of Straining or Loading," Materials and Structures, Volume 8, No. 44, pp. 108-116.

41.   McHenry, D, Shideler, J.J., "Review of Data on Effect of Speed in Mechanical Testing of Concrete," ASTM Special Technical Publication No. 185, pp. 72-82.

42.   Rasch, C., "Stress-Strain Curves of Concrete and Stress Distribution in the Flexural Compression Zone under Constant Strain Rate," (in German), Duetscher Ausschuss Für Stahlbeton, Bulletin No. 154, Berlin, 1962.

43.   Watstein, D, "Effect of Straining Rate on the Compressive Strength and Elastic Properties of Concrete," American Concrete Inst. Journal, Vol. 49, No. 8, April 1953, pp. 729-744.

44.   Watstein, D., "Properties of Concrete at High Speek of Loading," Symposium on Impact Testing, STP No. 176, ASTM, 1956, pp. 150-169.

45.   Bažant, Z.P., Asghari, A.A., "Constitutive Law for Nonlinear Creep of Concrete," J. of the Eng. Mech. Div., ASCE, Vol. 103, No. EM1, Proc. Paper 12729, Feb. 1977, pp. 113-124.

46.   Bažant, Z.P., Kim, S.-S., "Nonlinear Creep of Concrete-Adaptation and Flow" J. of the Engrg. Mech. Div., ASCE, Vol. 105, No. EM3, Proc. Paper 14654, June 1979, pp. 429-446.

47.   Bažant, Z.P., "Theory of Creep and Shrinkage in Concrete Structures: A Précis of Recent Developments," Mechanics Today, Vol. 2, Pergamon Press, Inc., New York, 1975, pp. 1-93.

48. Bažant, Z.P., Osman, E., "Double Power Law for Basic Creep of Concrete," Materials and Structures, Paris, France, Vol. 9, 1976, pp. 3-11.

49. Bažant, Z.P., Panula, L., "Prediction of Time-Dependent Deformations of Concrete," Materials and Structures, Paris, France, Parts I and II, Vol. 11, No. 65, 1978, pp. 307 - 328; Parts III and IV, Vol. 11, No. 66, 1978, pp. 415-434; Parts V and VI, Vol. 12, No. 69, 1979

50. Bažant, Z.P., "Critique of Orthotropic Models and Triaxial Testing of Concrete and Soils," Structural Engineering Report No. 79-10/640c, Northwestern University, Evanston, Illinois, October 1979.

51. Truesdell, C., "Hypo-elasticity," Journal of Rational Mechanics Analysis, Vol. 4, 1955, pp. 83-133.

52. Coon. M.D., Evans, R.J., "Incremental Constitutive Laws and their Associated Failure Criteria with Application to Plain Concrete," Int. J. of Solids and Structures, Vol. 8, 1972, pp. 1169-1180.

53. Bažant, Z.P., Tsubaki, T., "Concrete Reinforcing Net: Optimum Slip-Free Limit Design," J. of the Struct. Div., Proc. ASCE, Vol. 105, 1979, pp. 327-346; Discussion Vol. 106.

54. Bažant, Z.P., Tsubaki, T., "Slip-Dilatancy Model for Cracked Reinforced Concrete," J. of the Struct. Div. Proc., ASCE, Vol. 106, Sept. 1980, pp.

55. Baumann, T., "Zur Frage der Netzbewehrung von Flächentagwerken," Der Bauingenieur, Vol. 47, No. 10, 1972, pp. 367-377.

56. Brondum-Nielsen, T., "Optimum Design of Reinforced Concrete Shells and Slabs," Report No. R.44, Structural Research Laboratory, University of Denmark, Copenhagen, Denmark, 1974, pp. 190-200.

57. Duchon, N.B., Analysis of Reinforced Concrete Membrane Subject to Tension and Shear," American Concrete Inst. Journal, Proc. Vol. 69, No. 9, Sept. 1972, pp. 578-583.

58. Morley, C.T., "Skew Reinforcement of Concrete Slabs against Bending and Torsional Moments," The Institution of Civil Engineers, Proceedings, Vol. 42, Jan. 1969, pp. 57-74.

59. Buyukozturk, O., Leombruni, P., Connor, J., "Analysis of Shear Transfer in Reinforced Concrete with Application to Containment Wall Specimens," Research Report R72-26, Dept. of Civil Engineering, Massachusetts Institute of Technology, Cambridge, Mass, June 1979.

60. Fenwick, R.C., "The Shear Strength of Reinforced Concrete Beams, " thesis presented to the University of Canterbury, at Christchurch, New Zealand, in 1966, in partial fulfillment of the requirements for degree of Doctor of Philosophy.

61. Hofbeck, J.A., Ibrahim, I.O., and Mattock, A.H., "Shear Transfer in Reinforced Concrete," J. of the American Concrete Inst. Vol. 66, No. 13, Feb. 1969, pp. 119-128.

62. Houde, J. Mirza, M.S., "A Finite Element Analysis of Shear Strength of Reinforced Concrete Beams," Special Publication SP42, American Concrete Inst., 1974, pp. 103-128.

63. Paulay, T., Loeber, P.J., "Shear Transfer by Aggregate Interlock," Special Publication SP42, American Concrete Inst., 1974, pp. 1-15.

64. Jimenez-Perez, R., Gergely, P., White, R.N., "Shear Transfer Across Cracks in Reinforced Concrete," Report 78-4, Dept. of Structural Engineering, Cornell University, Ithaca, NY, Aug. 1978.

65. Mattock, A.H., "Shear Transfer in Concrete Having Reinforcement at an Angle to the Shear Plane," Special Publication SP42, American Concrete Inst., 1974, pp. 17-42.

66. Yuzugullu, O., Schnobrich, W.C., "A Numerical Procedure for the Determination of the Behavior of a Shear Wall Frame System," American Concrete Inst. Journal, Vol. 70, No. 7, July 1973, pp. 474-479.

67. Bažant, Z.P., and Gambarova, P.,"Rough Cracks in Reinforced Concrete," J. of the Struct. Div., Proc. ASCE, Vol. 106, 1980, pp. 819-842.

68. Bažant, Z.P., Tsubaki, T., Belytschko, T.B., "Concrete Reinforcing Net: Safe Design," J. of the Struct. Div., Proc. ASCE, Vol. 106, Sept. 1980, pp.

69. Marchertas, A.H., Fistedis, S.H., Bažant, Z.P., and Belytschko, T.B., Analysis and Application of Prestressed Concrete Reactor Vessels for LMFBR Containment, Nuclear Engng. and Design, Vol. 49, July 1978, pp. 155-173.

70. Cedolin, L., and Dei Poli, S., "Finite Element Studies of Shear-Critical R/C Beams," J. of the Engng. Mech. Div. ASCE, Vol. 103, No. 12968, June 1979, pp. 395-410.

71. Ngo, D., Scordelis, A.C., "Finite element Analysis of Reinforced Concrete Beams," J. of the American Concrete Inst., Vol. 66, No. 3, March 1967, pp. 152-153.

72. Scordelis, A.C., "Finite element Analysis of Reinforced Concrete Structures" Proceedings, Specialty Conf. on Finite Element Methods In Civil Engrg., McGill University, Montreal, Quebec, Canada, 1972, pp. 71-113.

73. Suidan, M., and Schnobrich, W.C., "Finite Element Analysis of Reinforced Concrete," J. of the Struct. Div., ASCE, Vol. 99, No. ST10, Proc. Paper 10081, Oct. 1973, pp. 2109-2122.

74. Bažant, Z.P., "Instability, Ductility, and Size Effect in Strain-Softening Concrete," J. of the Engineering Mech. Div., ASCE, Vol. 102, No. EM2, Proc. Paper 12042, April 1976, pp. 331-344.

75. Bažant, Z.P., Cedolin, L., "Blunt Crack Band Propagation in Finite Element Analysis," J. of the Eng. Mech. Div., Proc. ASCE, Vol. 105, No. EM2, April 1979, pp. 297-315.

76. Bažant, Z.P., Cedolin, L., "Fracture Mechanics of Reinforced Concrete," Structural Engng. Report No. 79-9/640m, Dept. of Civil Engineering, Northwestern University, Sept. 1979, to also appear in Journal of the Struct. Div., ASCE.

77. Cedolin, L. and Bažant, Z.P., "Effect of Finite Element Choice in Blunt Crack Band Analysis," Struct. Engineering Report No. 79-6/640e, Dept. of Civil Engineering, Northwestern Univ., June 1979, also Computer Methods in Applied Mechanics and Engineering, 1980, in press.

78. Rice, J.R., "Mathematical Analysis in the Mechanics of Fracture," Fracture, an Advanced Treatise, H. Liebowitz, ed., Vol. 2, Academic Press, New York, 1968, pp. 191-250.

79. Hawkins, N.M., Wyss, A.N. and Mattock, A.H., "Fracture Analysis of Cracking in Concrete Beams," J. of the Struct. Div., ASCE, Vol. 103, No. ST5, Proc. Paper 12921, May, 1977, pp. 1015-1030.

80. Kaplan, M.F., "Crack Propagation and the Fracture of Concrete," American Concrete Inst. Journal, Vol. 58, No. 11, Nov. 1961.

81. Shah, S.P., McGarry, F.J., "Griffith Fracture Criterion and Concrete," J. of the Engrg. Mech. Div., ASCE, Vol. 97, No. EM6, Proc. Paper 8597, Dec. 1971, pp. 1163-1976.

82. Walsh, P.F., "Fracture of Plain Concrete," The Indian Concrete Journal, Vol. 46, No. 1972, pp. 469, 470, and 476.

Leere Seite

Blank page

Page vide